

# Evaluating stony coral tissue loss disease intervention success through whole-transcriptome gene expression profiling

Michael Studivan<sup>1</sup>, Ryan Eckert<sup>2</sup>, Erin Shilling<sup>1</sup>, Nash Soderberg<sup>3</sup>, Ian Enochs<sup>4</sup>, and Joshua Voss<sup>1</sup>

<sup>1</sup>Florida Atlantic University

<sup>2</sup>Harbor Branch Oceanographic Institute

<sup>3</sup>University of Miami Rosenstiel School of Marine and Atmospheric Science

<sup>4</sup>NOAA Atlantic Oceanographic and Meteorological Laboratory

February 11, 2023

## Abstract

Stony coral tissue loss disease (SCTLD) remains an unprecedented disease outbreak due to its high mortality rate and rapid spread throughout Florida’s Coral Reef and wider Caribbean. A collaborative effort is underway to evaluate disease intervention strategies that mitigate the spread of SCTLD across coral colonies and reefs. We conducted an in-situ experiment in Southeast Florida to assess molecular responses among SCTLD-affected *Montastraea cavernosa* pre- and post-application of the most widely-used intervention method, CoreRx Base 2B with amoxicillin. Through Tag-Seq gene expression profiling of apparently healthy, diseased, and treated corals, we identified modulation of metabolomic and immune pathways following antibiotic treatment. In a complementary ex-situ disease challenge experiment, we exposed nursery-cultured *M. cavernosa* and *Orbicella faveolata* fragments to SCTLD-affected donor corals to compare transcriptomic profiles among clonal individuals from unexposed controls, those exposed and displaying disease signs, and corals exposed and not displaying disease signs. Suppression of metabolic functional groups and activation of stress gene pathways as a result of SCTLD exposure were apparent in both species. Amoxicillin treatment led to a ‘reversal’ of the majority of gene pathways implicated in disease response, suggesting potential recovery of corals following antibiotic application. In addition to increasing our understanding of molecular responses to SCTLD, we provide resource managers with transcriptomic evidence that disease interventions with antibiotics appear to be successful and may help to modulate coral immune responses to SCTLD. These results contribute to feasibility assessments of intervention efforts following disease outbreaks and improved predictions of coral reef health in Southeast Florida.

## Introduction

Since its first observation near Miami, Florida in 2014, stony coral tissue loss disease (SCTLD) has spread throughout Florida’s Coral Reef and to at least 25 jurisdictions across the wider Tropical Western Atlantic (Kramer et al., 2019; NOAA, 2018; Precht et al., 2016). The disease affects at least 24 scleractinian species and is characterized by subacute to acute tissue loss leading to colony mortality, often with formation of rapidly-progressing focal or multifocal lesions (G. Aeby et al., 2021; G. S. Aeby et al., 2019; Landsberg et al., 2020; NOAA, 2018). The pathogen(s) have not yet been identified, though examination of microbiomes of diseased samples suggest a bacterial (Becker et al., 2021; Meiling et al., 2021; Meyer et al., 2019; Rosales et al., 2020, 2022; Studivan et al., 2022; Ushijima et al., 2020) and/or viral (Veglia et al., 2022; Work et al., 2021) consortium. Antibiotic treatments have shown high rates of success in halting the progression of disease lesions, and in some cases, the quiescence of visible disease signs on treated colonies (Forrester et al., 2022; Neely et al., 2020; Shilling et al., 2021; Walker et al., 2021). Attempts to treat SCTLD-affected corals with chlorinated epoxy, which was hypothesized to affect more potential pathogenic taxa relative to targeted antibiotics, have been largely unsuccessful (Shilling et al., 2021; Walker et al., 2021). The mechanisms by

which antibiotic application affects disease progression are unknown, particularly the potential impacts on the coral host and its microbiome in processes such as recovery and potential antibiotic resistance.

The molecular mechanisms underlying coral immune responses to SCTL D are poorly understood relative to other diseases (Traylor-Knowles et al., 2022). A recent study utilizing an untargeted metabolomic approach identified several lipid and tocopherol classes of Symbiodiniaceae origin that distinguished healthy and diseased corals, providing further evidence of algal symbiont involvement in SCTL D (Deutsch et al., 2021). Transcriptomic approaches have also been used to examine gene expression of disease lesion tissue in the coral species *Montastraea cavernosa* and *Orbicella faveolata*, finding differential expression of numerous genes implicated in stress, extracellular matrix rearrangement, immunity, and apoptosis pathways (Traylor-Knowles et al., 2021). Relatively few similarities, however, were observed between coral species, indicating a need for additional cross-species comparisons to identify consistent disease response mechanisms. To date no transcriptomic studies of SCTL D, or any coral disease, have focused on the effects of intervention methods, identifying a critical need to understand the potential consequences of antibiotic treatment of host and symbiont responses.

To address this knowledge gap, we conducted paired ex-situ transmission and in-situ intervention experiments, and examined whole-transcriptome gene expression patterns of corals in response to disease exposure and antibiotic treatment, respectively. These experiments focused on the coral species *M. cavernosa* and *O. faveolata* due to their ongoing use in field-based disease intervention and monitoring efforts (Shilling et al., 2021; Walker et al., 2021), ecological importance as primary reef-builders (González-Barrios & Álvarez-Filip, 2018; Walton et al., 2018), and growing use in reef restoration (Koval et al., 2020; Rivas et al., 2021). Through these experiments, we 1) identified transcriptomic responses to SCTL D exposure in a controlled lab setting, 2) compared responses to disease exposure between species, 3) examined transcriptomic modulation following antibiotic treatment in a field-based time series, and 4) compared trends between diseased and treated corals in lab and field settings. In doing so we seek to better understand coral immune responses to SCTL D, and to provide transcriptomic resources to the development of disease exposure diagnostics. These experiments also evaluated disease intervention effectiveness at the molecular level and identified potential patterns of recovery following treatment of SCTL D-affected wild colonies with antibiotics.

## Methods

### Transmission experiment

The ex-situ transmission experiment was conducted in the Experimental Reef Laboratory at the University of Miami's Cooperative Institute for Marine and Atmospheric Studies over a period of two weeks in March 2020. The disease transmission apparatus consisted of 80, 0.5 L coral vessels with independent flow-through water sources maintained at local ambient temperature (24 °C) and light conditions (PAR of 250  $\mu\text{mol m}^{-2}\text{s}^{-1}$ ; Studivan et al., 2022). Twenty fragments each of disease-naïve *O. faveolata* and *M. cavernosa* were sourced from the land-based nursery at Mote Marine Laboratory. Each fragment was split into two equal subfragments for healthy/disease exposure genotype pairs ( $N = 80$  total) and allowed to recover for eight days prior to the disease challenge. A disease donor colony of *M. cavernosa* with visible SCTL D lesions was collected from Broward County, Florida (26.1479, -80.0939) two days prior to the start of the experiment, and was cut into  $\sim 1 \times 4$  cm fragments using a diamond band saw with each fragment containing a portion of active lesion. Coral fragments in the disease-exposed group were maintained in direct contact with diseased tissue fragments, where disease donor fragments were replaced as needed following total loss of tissue. Genotype pairs in the healthy group were not exposed to any other corals. Corals were observed daily over the course of the experiment to quantify the number of days to onset of disease lesions, as well as to observe the gross signs of lesion formation and tissue necrosis. Following progression of lesions across approximately 50% of the fragment area, coral fragments and their corresponding healthy genotype pair were sampled via a small tissue scrape from near the lesion, which was preserved in TRIzol and flash-frozen in liquid nitrogen. Corals remaining at the end of the experiment were processed in the same manner. Herein, coral fragments are characterized as “healthy” for all samples in the control group, “diseased” for samples in the disease-exposed group exhibiting lesions, and “NAI” (no active infection) for samples in the disease-exposed group that

showed no visible signs of disease lesions by the end of the experiment.

### Intervention experiment

The in-situ intervention experiment was conducted at long-term monitoring site BC1 (mean depth 5.8 m) in Broward County, Florida (26.1479, -80.0939; Combs et al., 2021; Shilling et al., 2021) over thirteen days in April–May 2020. Fifteen colonies of *M. cavernosa* with visible SCTL D lesions were tagged and small tissue scrapes were collected 5 cm from the disease lesion and preserved as described previously. Nineteen visually healthy colonies of the same species were also tagged and sampled. Following the initial sampling, diseased colonies were treated with amoxicillin in CoreRx Base 2B as described in Shilling et al. (2021), with the exception that trenching of the coral skeleton in advance of the disease lesion was not conducted. Colonies were then revisited thirteen days later, and tissue sampling was repeated.

### Tag-Seq library preparation, sequencing, and bioinformatics

Total RNA was extracted from samples from both experiments using modified versions of protocols for the Zymo Direct-zol RNA Miniprep and Zymo RNA Clean & Concentrator-5 kits (Studivan, 2022d). RNA was quantified on an Agilent Bioanalyzer 2100 and analyzed for purity on a Nanodrop 1000, where samples with RIN scores <4, or poor purity ratios, were re-extracted. All successfully-extracted samples were normalized to 60 ng/μL and shipped to the University of Texas at Austin Genome Sequencing and Analysis Facility for library preparation and sequencing. Tag-Seq library preparation was performed in duplicate using 600 ng of initial RNA for *M. cavernosa* samples and 100 ng for *O. faveolata* samples due to initial issues with inhibitory compounds. Following successful amplification of all samples, libraries were pooled and sequenced on a NovaSeq 6000 S2-XP flow cell generating 1 x 100 bp reads with 20% *PhiX* spike-in, for a target read depth of ~10 million reads per library (~20 million reads per sample).

Raw sequences were processed according to custom Perl scripts in a GitHub repository release (Studivan, 2022d) to deduplicate, trim (FASTX-Toolkit; Gordon & Hannon, 2010), align (Bowtie 2; Langmead & Salzberg, 2012), and quantify gene counts for each sample. Dominant symbiont genera were determined by aligning sample reads to a reference containing Symbiodiniaceae 28S sequences across the four main genera (*Symbiodinium* spp., *Breviolum* spp., *Cladocopium* spp., and *Durusdinium* spp.). *Orbicella faveolata* samples contained a majority of *Durusdinium* spp. alignments (93.4%), and *M. cavernosa* samples were dominated by *Cladocopium* spp. (99.7%); hence, the respective species datasets were aligned to the dominant symbiont references. Cleaned reads were mapped to separate host (*M. cavernosa*, Kitchen et al., 2015; *O. faveolata*, Pinzón et al., 2015) and algal symbiont (*Cladocopium* spp., Davies et al., 2018; *Durusdinium* spp., Shoguchi et al., 2021; respectively) reference transcriptomes sequentially to remove cross-contaminated sequences in both host and symbiont transcriptomes. Transcriptome annotations for host and symbiont references were created according to GitHub repositories for *O. faveolata* (Studivan, 2022b) and *M. cavernosa* (Studivan, 2022a) using eggNOG-Mapper (Huerta-Cepas et al., 2016, 2018).

Following deduplication, the mean number of reads across all samples was  $24.6 \pm 0.9$  million, with  $5.8 \pm 0.2$  million reads remaining following trimming and cleaning. Alignment rates for *O. faveolata* samples were  $60.3 \pm 1.6\%$  for host and  $15.6 \pm 0.8\%$  for symbionts, resulting in 81,960 and 39,854 isogroups, respectively. For *M. cavernosa* samples, alignment was  $61.2 \pm 0.7\%$  for host and  $6.5 \pm 0.3\%$  for symbionts, with 82,594 and 32,862 isogroups, respectively. The original version of the *M. cavernosa* transcriptome was chosen over the updated, genome-derived version (<https://matzlab.weebly.com/data-code.html>) due to low alignment in the latter ( $28.0 \pm 0.3\%$  for host and  $7.1 \pm 0.4\%$  for symbiont) and poorer representation of isogroups (24,850 and 32,932 isogroups, respectively) for downstream differential expression analysis.

### Statistical analysis

All statistical analyses were conducted in the R statistical environment (R Core Team, 2019). Analysis scripts and outputs can be found in a GitHub repository release associated with this manuscript (Studivan, 2022c). Transmission metrics from the transmission experiment (time to onset of disease lesions) were analyzed for an effect of species using an ANOVA of Box-Cox transformed data, and with a fit proportional hazards regression

model in the packages *survival* (Therneau, 2021) and *survminer* (Kassambara et al., 2021) to determine the relative risk of developing disease lesions between species.

Gene counts were first separated by experiment, species, and host/symbiont datasets, then pre-filtered to remove isogroups with a cumulative count  $<10$  across all samples. Data were subsequently transformed using a variance stabilizing transformation in the *DESeq2* package (Love et al., 2014), and examined for outlier samples using the package *arrayQualityMetrics* (Kauffmann et al., 2009). Samples violating the distance between sample arrays criterion ( $S_a$ ) were removed from the respective experiment and host/symbiont datasets (Table 1; Table 2). Significance testing for each experiment dataset was performed with PERMANOVAs using  $1e^6$  permutations, and sample dispersion was visualized using PCoAs of Manhattan distance in the package *vegan* (Oksanen et al., 2015). Differential expression analyses were conducted using *DESeq2* models for the respective experiments. For *O. faveolata* in the transmission experiment, the model genotype + exposure group (control, sctld) was used, whereas for *M. cavernosa*, the model genotype + disease status (healthy, diseased, NAI) was used since not all fragments exhibited disease signs. For the intervention experiment, a single-factor concatenated treatment (control, SCTLD) and time (0,1) model was used. Contrast statements to conduct pairwise comparisons for each of the experiment datasets as described in the GitHub repository release (Studivan, 2022c). Visualization of differentially expressed genes (DEGs) was done using the *pheatmap* package (Kolde, 2019).

Functional enrichment analyses with Mann-Whitney  $U$  tests were conducted for each experiment’s pairwise comparisons using the packages *GO-MWU* (Wright et al., 2015) with an alpha cutoff of 0.05 and *KOGMWU* (G. B. Dixon et al., 2015) for full gene ontology (GO) and eukaryotic orthologous group (KOG) annotations, respectively. To identify correlational relationships between gene modules (genes with similar expression patterns) and experimental variables, weighted gene co-expression network analyses (WGCNA; Langfelder & Horvath, 2008) were conducted as described in the associated GitHub repository release (Studivan, 2022c). Module-associated genes were then exported for GO enrichment analysis to examine any relationships between gene expression patterns and additional sample traits beyond diseased versus healthy status.

Finally, DEGs unique to and shared between species and experiments were determined using the *VennDiagram* package (Chen & Boutros, 2011). For the transmission experiment, common DEGs (orthogroups) and associated GO/KOG annotations for diseased/healthy comparisons in *O. faveolata* and *M. cavernosa* were identified by blast annotations using OrthoFinder (Emms & Kelly, 2015, 2019), and visualized by heatmaps and KOG classes. For comparison of DEGs in *M. cavernosa* samples from the transmission and intervention experiments (e.g., to compare DEGs in disease-exposed transmission samples to antibiotic-treated samples in the intervention experiment), matching gene and KOG annotations were examined in the same fashion as the cross-species comparisons.

## Results

### Transmission experiment

There was a significant difference in the number of days to the onset of visible disease lesions between species (ANOVA:  $F_{1,29} = 6.22$ ,  $p < 0.019$ ), with *O. faveolata* significantly more likely to develop SCTLD lesions compared to *M. cavernosa* (log-rank:  $z_{1,29} = 3.569$ ,  $p < 0.001$ ; Figure S1). Transmission rates in the disease-exposed treatment at the conclusion of the experiment were 95% for *O. faveolata* with lesions occurring at a mean of  $3.1 \pm 0.5$  days, while 55% of *M. cavernosa* fragments exhibited lesions at a mean of  $5.4 \pm 1.0$  days (Table 1). No controls in either species developed lesions. Signs of SCTLD were similar between species, with tissue necrosis and lesion formation/progression being the most common (Dataset S1).

Two-way PERMANOVAs identified significant effects of coral genotype and disease status for *M. cavernosa* and associated *Cladocopium* datasets, while the effects of genotype and exposure group were marginally insignificant for *O. faveolata* ( $p = 0.057$  and  $p = 0.056$ , respectively) and nonsignificant for associated *Durusdinium* symbionts (Table 3). Pairwise differential expression tests with *DESeq2* indicated the majority of differentially expressed genes (DEGs) to be attributed to diseased versus healthy samples for *M. cavernosa* (3,890 upregulated and 3,878 downregulated), with 1,820 DEGs between diseased and samples

not exhibiting visible disease signs following exposure (NAI; 960 upregulated and 860 downregulated), and 115 DEGs between NAI and healthy samples (43 upregulated, 72 downregulated). Few DEGs were identified for any pairwise comparisons in *Cladocopium* symbionts, with five in diseased versus healthy samples and two in NAI versus healthy samples. *Orbicella faveolata* showed moderate numbers of DEGs between diseased and healthy samples (385 upregulated and 188 downregulated), with no DEGs for *Durusdinium* (Table 4). Ordination with PCoAs demonstrated that diseased samples were distinct from all other samples for *M. cavernosa*, while NAI and healthy samples were more similar (Figure 1). This relationship was reversed for *Cladocopium* data, where diseased and NAI samples were more closely related to each other than to healthy samples. Both *O. faveolata* and *Durusdinium* samples showed similarities between healthy and diseased samples, with little differentiation between exposure groups in the ordination space (Figure 1).

Functional enrichment analysis using gene ontology (GO) identified 434 GO terms across three categories (molecular function [MF]: 38; biological process [BP]: 287; cellular component [CC]: 109) for diseased versus healthy *M. cavernosa* samples, and 45 GO terms for *O. faveolata* (MF: 9; BP: 20; CC: 16; Table S1). The majority of enriched GO terms were negatively represented in diseased *M. cavernosa*, while the opposite was true for *O. faveolata*. For diseased versus NAI *M. cavernosa*, 371 GO terms were significantly enriched (MF: 50; BP: 244; CC: 77), while only 8 terms were significantly enriched for NAI versus healthy samples (BP: 2; CC: 6; Table S2). No GO terms were significantly enriched for *Cladocopium* or *Durusdinium* symbionts, however. Functional enrichment of eukaryotic orthologous groups (KOGs) demonstrated similar patterns between diseased versus healthy and diseased versus NAI samples for *M. cavernosa* (Figure S2), where metabolic and transport mechanisms were generally downregulated in diseased samples, and nuclear structure and translation-related pathways were upregulated. Some nuclear structure and membrane pathways were positively enriched in NAI versus healthy *M. cavernosa*, with down regulation of translation, cytoskeleton, and extracellular pathways. *Cladocopium* diseased and NAI samples showed mild enrichment of most pathways relative to healthy controls, with nuclear structure as the most positively enriched, and cell motility as the most downregulated. Similar trends were observed for diseased versus healthy *O. faveolata* as compared to *M. cavernosa*, while *Durusdinium* showed an inverse pattern of KOG enrichment in diseased samples relative to *Cladocopium* (Figure S2).

Weighted gene coexpression network analysis (WGCNA) identified ten modules with significant correlations to experimental factors (disease status and the time to onset of lesions). In general, modules that were negatively correlated with healthy samples were positively correlated with diseased samples (Figure S3). Several modules were also correlated with NAI samples that demonstrated similar expression to diseased samples ('darkorange2') and the time to transmission ('thistle1' and 'darkorange2'), or inverse relationships with healthy samples ('navajowhite1'). Of the modules correlated with NAI samples, only 'darkorange2' showed significant GO enrichment to the mRNA metabolic process (BP) and peptidase, cytosolic, and ribosomal complexes (CC; Table S4). Four modules were found to have significant trait correlations for *Cladocopium*, with similar expression patterns between NAI and diseased samples relative to healthy controls in the 'pink' module, but no significant GO enrichment (Table S4). The *O. faveolata* dataset had six modules with significant correlations to disease status and the time to onset of lesions; most of these were inversely related between diseased and healthy samples, apart from the 'tan' module that was inversely related between NAI and healthy samples (Figure S3). There were no significantly enriched GO terms for the 'pink' or 'tan' modules correlated with NAI samples. WGCNA was not successful in assigning modules to the *Durusdinium* dataset. Module hub genes (i.e., genes with the highest module membership) were largely unannotated for the respective reference datasets, with no apparent relationship between coral species or among associated symbionts (Table S3).

Orthofinder identified 681 orthologous DEGs in diseased versus healthy samples; of these, 438 showed similar expression patterns between species (272 upregulated and 166 downregulated), and 243 showed inverse expression (Figure 2). While expression of individual genes was in some cases inversely related between species, the corresponding KOG annotations demonstrated that the number of DEGs within each KOG class that was up- or downregulated was relatively similar, suggestive of an overall similar function response to disease exposure between *M. cavernosa* and *O. faveolata*. Likewise, examination of GO categories in diseased

versus healthy samples indicated 21 GO terms (MF: 2; BP: 11; CC: 8) that were commonly enriched in the same direction between species (Table 5; Figure 3).

### Intervention experiment

PERMANOVAs indicated no significant effect of time or treatment on the gene expression of *M. cavernosa* or associated *Cladocopium* symbionts (Table 3). Visualization with PCoA revealed overlapping sample dispersion in the coral and symbiont ordinations (Figure 4). Differential expression analyses, however, identified DEGs associated with pairwise treatment/time comparisons, with a high number of DEGs between diseased and healthy corals at  $t_0$  (410 DEGs: 284 upregulated and 126 downregulated), as well as between amoxicillin-treated corals at  $t_1$  and their original diseased state at  $t_0$  (241 DEGs: 48 upregulated and 193 downregulated; Table 4; Figure 4). There were few differences between treated and healthy corals at  $t_1$  (5 DEGs: 4 upregulated and 1 downregulated) and temporal shifts in gene expression were evident (e.g., 248 DEGs in  $t_1$  versus  $t_0$  healthy corals). Few DEGs were identified across pairwise comparisons for *Cladocopium* (Table 4; Figure 4).

Functional enrichment analysis identified 46 significantly enriched GO terms in diseased versus healthy corals at  $t_0$  (MF: 9; BP: 10; CC: 27), 39 GO terms in treated versus diseased corals (MF: 6; BP: 14; CC: 19), and 7 GO terms in treated versus healthy corals at  $t_1$  (MF: 1; CC: 6; Table S5). Similar to *M. cavernosa* samples from the transmission experiment, the majority of enriched GO terms were negatively enriched in diseased versus healthy corals. Conversely, treated corals showed positive enrichment of most GO terms relative to healthy controls at  $t_1$ . KOG enrichment in diseased versus healthy corals at  $t_0$  was similar to the trends observed for the transmission experiment, where several metabolic and transport pathways were negatively enriched (Figure S4). Notably, the nuclear structure KOG class was highly negatively enriched in diseased corals, where it was shown to be positively enriched for both diseased *M. cavernosa* and *O. faveolata* samples from the transmission experiment. Comparison of treated versus diseased corals demonstrated an opposite response in the same pathways as compared to diseased versus healthy corals, showing an increase in metabolic, transport, and nuclear structure classes. No KOG classes were strongly enriched when comparing treated and healthy corals at  $t_1$ . *Cladocopium* KOG enrichment was similar in diseased versus healthy corals to the transmission experiment samples, with strong positive enrichment of the nuclear structure class and negatively enrichment of cell motility. Following treatment with amoxicillin, those patterns were reversed, even when comparing treated to healthy corals at  $t_1$  (Figure S4).

WGCNA returned 8 modules significantly correlated with treatments/time points, with the strongest patterns of correlation reversal between healthy corals at  $t_0$  to  $t_1$  (modules ‘darkred’ and ‘salmon;’ Figure S5). Modules ‘greenyellow’ and ‘purple’ showed inverse correlations between diseased and healthy corals at  $t_0$ , and only the ‘pink’ module showed an inverse relationship between treated and diseased corals. Only the ‘darkred’ module contained significantly enriched GO terms, all of which were related to endoplasmic reticulum complexes (CC; Table S4). One module had a significant correlation to experimental traits in *Cladocopium*, but it was driven by one sample and therefore disregarded. Visualization of expression patterns for the 30 most significant DEGs in modules ‘greenyellow’ and ‘grey60’ demonstrated a shift in expression patterns from the original disease state being distinct to healthy controls, to overall similarities between treated and healthy corals (Figure S5). Of the module hub genes with annotations, none matched among reference transcriptomes for the transmission experiment, although the ‘green’ module hub gene belongs to the heat shock protein 70 family (Table S3).

### Cross-experiment comparisons

Comparison of diseased versus healthy samples from the transmission and intervention experiments revealed 1,458 genes that were shared between experiments. The majority of common genes showed the same directionality between experiments (452 upregulated and 489 downregulated), while 517 genes showed inverse relationships between experiments (Figure 5). When comparing diseased versus healthy samples in the transmission experiment to treated versus diseased corals in the intervention experiment, however, the majority of genes were found in inverse relationships between experiments (1,041 genes), whereas only 285 genes were found to share the same direction of expression (121 upregulated and 164 downregulated). Gene

representation within KOG classes was largely similar across experiments, with the exception of unannotated genes that contributed to variability between experiments and among disease status/treatment comparisons (Figure 5).

## Discussion

### Strong transcriptional responses to SCTL D exposure in both coral species

Exposure to stony coral tissue loss disease in these experiments caused evident transcriptional responses in both coral species. In general, we observed a depression of host metabolic pathways and a corresponding increase in expression of stress response genes and nuclear processes (Figure S2). This is unsurprising given consistency in transcriptomic responses to myriad stressors, a phenomenon characterized as a conserved stress response among diverse coral taxa (G. Dixon et al., 2020; Wang et al., 2009). While there was evidence of a strong transcriptional response to disease exposure in host corals, there was little variation in the transcriptional response of symbionts in both experiments. This may be due to lower alignment rates to the symbiont transcriptomes relative to the coral hosts ( $6.5 \pm 0.3\%$  for *Cladocopium* and  $15.6 \pm 0.8\%$  for *Durusdinium* versus  $61.2 \pm 0.7\%$  for *M. cavernosa* and  $60.3 \pm 1.6\%$  for *O. faveolata*, respectively), or comparatively poor annotations in symbiont references. Therefore, we have focused primarily on interpretation of the coral host datasets to minimize speculation with the symbiont datasets.

Through comparative analyses between coral species in the transmission experiment, we found consistent overlap in transcriptional responses following exposure to SCTL D. There were 681 DEGs and 21 GO terms shared between disease-exposed *M. cavernosa* and *O. faveolata* (Figures 2; 3), which may be an underestimation of orthologous genes between species, since some orthogroups had different gene-level annotations. The majority of DEGs (~64%) and all GO terms were expressed or enriched in the same direction in response to SCTL D exposure, suggesting that there are many conserved pathways among coral species functioning in the same roles. This relationship has been corroborated in a recent study by MacKnight and colleagues (2022), which examined transcriptional responses of seven coral species (including our study species) to white plague disease. They reported expression of immunity and cytoskeletal arrangement gene pathways across all species following disease exposure, with variation in intracellular protein trafficking pathways related to differences between disease susceptibility among and within species. Similarly, we observed higher enrichment of protein trafficking GO and KOG terms in *M. cavernosa*, which is less susceptible to SCTL D than *O. faveolata* (Figure 3; Figure S2) (Meiling et al., 2021; NOAA, 2018).

Conversely, a minority of DEGs showed inverse relationships between species following exposure to SCTL D (Figure 2). Despite this, functional enrichment of GO and KOG terms were largely similar between species (Figure 3; Figure S2), potentially indicating modulation of conserved gene pathways between *M. cavernosa* and *O. faveolata* (i.e., different species using the same gene pathways in different ways). This modulation may be indicative of plasticity related to disease susceptibility (e.g., MacKnight et al., 2022), and warrants additional investigation with other species affected by SCTL D.

Traylor-Knowles and colleagues (2021) identified differentially expressed gene processes implicated in coral immunity following exposure to SCTL D. In this study, we observed 26 DEGs in SCTL D-exposed *M. cavernosa* associated with these same immune processes, and 19 DEGs in *O. faveolata*. These included two apoptosis regulation pathways that were differentially expressed in *M. cavernosa* only, which are implicated in cell death and necrosis (D’Arcy, 2019; Fuess et al., 2017). Extracellular matrix genes (four for *M. cavernosa* and three for *O. faveolata*) were generally downregulated in both species, and are hypothesized to be related to wound healing and the prevention of lesion progression (Traylor-Knowles et al., 2021; Young et al., 2020). Four transforming growth factor-beta (TGF- $\beta$ ) DEGs were downregulated in *M. cavernosa* only, which are likely part of the coral’s immune response (Fuess et al., 2020; Traylor-Knowles et al., 2021). Two NF- $\kappa$ B activation genes for each species were upregulated (though one *M. cavernosa* DEG was downregulated), where this transcription factor is well-known for its role in immune activation and potentially in regulation of the coral-algal symbiosis (Voolstra et al., 2009; Williams et al., 2018). This is perhaps related to the hypothesis that SCTL D may be a virus targeting Symbiodiniaceae (Veglia et al., 2022; Work et al., 2021),

but this observation requires further study.

Four peroxidases were upregulated in *M. cavernosa*, but ten DEGs had variable expression levels in *O. faveolata*. Peroxidases have been shown to be a component of the innate immune response to disease and thermal stress (Mydlarz & Harvell, 2007; Palmer, 2018). Protein tyrosine kinase (PTK) genes, which promote inflammatory responses to pathogens in corals (Fuess et al., 2016), had variable expression levels (nine in *M. cavernosa* and three in *O. faveolata*), corroborating that cytokine production may play a role in the response to SCTLD exposure (Traylor-Knowles et al., 2021). Finally, one WD-repeat gene per species was downregulated, which is likely involved in apoptotic and immune responses (Aranda et al., 2011). While these genes do not provide the complete picture of coral’s transcriptomic responses to SCTLD, their differential expression in both studies provides evidence of their importance in the immune response to this disease and may be useful in the identification of biomarkers of disease exposure in wild corals.

#### Effects of antibiotic treatments on coral transcriptional patterns

Treatment of corals with amoxicillin appears to result in a ‘normalization’ of transcriptional pathways associated with the response to SCTLD. When comparing expression profiles across all genes, treated corals appeared more similar to apparently-healthy controls than they did their original diseased state (Figure 4). Comparisons of diseased versus healthy samples in both transmission and intervention experiments revealed mostly similar patterns, with downregulation of metabolic pathways and upregulation of stress response, immune, and nuclear processes (Figure S4). The majority of shared DEGs between diseased individuals in both experiments were expressed in the same direction (~64%), however, examination of treated versus diseased colonies showed an inverse relationship of expression patterns across the majority of shared DEGs (~76%, Figure 5). This implies a reversal of the same transcriptomic mechanisms involved in the immune response to SCTLD following treatment with amoxicillin, and provides evidence that disease intervention may be beneficial to the coral beyond removal of potential pathogens and co-occurring opportunistic microbes that may be affecting host transcription. As studies evaluating the effectiveness of antibiotic treatments on diseased corals often focus on visible observations (i.e., lesion progression and/or quiescence; Forrester et al., 2022; Neely et al., 2020; Shilling et al., 2021; Walker et al., 2021) or shifts in microbial communities (Sweet et al., 2011, 2014) as a means of assessing treatment success, this hypothesis requires further testing to elucidate the impacts of antibiotic treatment on other members of the holobiont including the coral host. For example, antibiotics have additional immune-modulating and anti-inflammatory impacts on humans beyond alteration of associated microbial communities (Pradhan et al., 2016), which may prove beneficial to corals affected by SCTLD.

Examination of the SCTLD-associated immune responses described by Traylor-Knowles and colleagues (2021) in our datasets also corroborated the reversal of transcriptional patterns following amoxicillin treatment. Eleven immune-related pathways were differentially expressed in diseased versus healthy corals, with fourteen in treated versus diseased corals. While overlap was minimal between treatment comparisons (four identical DEGs), expression patterns were often inversely related among immune classes. Four extracellular matrix genes were upregulated in treated colonies compared to downregulated in diseased samples from the transmission experiment (no DEGs were observed for diseased versus healthy colonies in the intervention experiment). Two NF- $\kappa$ B activation DEGs were found for each treatment comparison and were upregulated in diseased versus downregulated in treated colonies. Three PTK genes were upregulated in diseased colonies while two matching genes (and one additional) were downregulated following treatment. TGF- $\beta$  and WD-repeat DEGs were also inversely-expressed between diseased and treated colonies, indicative of a shift in immune responses following antibiotic treatment.

#### Evaluation of antibiotic treatment as an SCTLD intervention

Amoxicillin is effective at slowing or halting SCTLD lesion progression on individual colonies, including in a field setting (Forrester et al., 2022; Neely et al., 2020; Shilling et al., 2021; Walker et al., 2021). There are multiple limitations of antibiotic effectiveness on broad-scale disease intervention efforts, including that this approach often requires multiple re-treatments, continuous monitoring, and is labor-intensive (Neely et

al., 2020; Walker et al., 2021). The time investment is especially important when considering reef systems with substantially more corals than southeast Florida, such as the Flower Garden Banks that recently experienced its first potential signs of a SCTLD outbreak (Johnston et al., 2023). While application of amoxicillin shows a high rate of success (~95%) in halting individual lesions, it does not necessarily prevent the formation of new lesions on a treated colony through time (e.g., Shilling et al., 2021). Finally, it is currently unknown what impacts antibiotic application may have on diverse coral reef ecosystems, notably potential antibiotic resistance in microbial communities (Griffin et al., 2020; Liu et al., 2020). Antibiotic treatment may additionally have negative impacts on healthy coral microbiomes, potentially increasing susceptibility of corals to other stressors such as elevated temperatures (Connelly et al., 2022).

Alternative treatment approaches are therefore warranted for further investigation in the mitigation of SCTLD, as well as future coral disease outbreaks. In particular, probiotic treatments are gaining research interest due to their potential benefits to coral survival following disease exposure (Peixoto et al., 2021), thermal stress (Doering et al., 2021; Santoro et al., 2021), and exposure to pollutants (Silva et al., 2021). Probiotic treatments are in development for SCTLD (Deutsch et al., 2022), and field trials are necessary to assess treatment effectiveness in a reef environment (Peixoto et al., 2021). Phage therapy also shows promise for the treatment of bacterial pathogens that affect corals (Jacquemot et al., 2018; Teplitski & Ritchie, 2009; Thurber et al., 2020), but many of these approaches are not yet fully operational.

While treatment of individual coral colonies with antibiotics is not intended to be a long-term solution to curbing the spread of SCTLD, it may represent a feasible method of mitigating impacts on high-value conservation and restoration targets, particularly ecologically-important, rare, and reproductively-viable members of the population. This is of particular importance while disease diagnostics are still being developed for SCTLD and other diseases. Disease diagnostics, when operational and scalable, may instead allow broad mitigation of pathogen transport via disease vectors and sources, potentially eliminating the need for colony-level disease intervention. Continued examination of gene mechanisms and functions will also improve understanding of coral immune responses (Traylor-Knowles et al., 2022), facilitating targeted treatment approaches in future disease outbreaks. Disease response efforts focusing on identification and diagnosis, mitigation of spread, and treatment of affected individuals require a holistic understanding of coral immunity and resilience at the individual level in order to maximize conservation and restoration success at the population level.

## Conclusions

Through complementary studies examining the transcriptomic responses of corals to SCTLD and subsequent antibiotic treatment, we identified a consistent signature of immune responses in both coral species examined. Further, we observed evidence of a reversal in immune responses related to disease exposure when corals were treated with amoxicillin, suggestive of a recovery process that may be occurring at the host level. Continued fate-tracking on treated corals is warranted to determine whether such gene expression patterns continue, with treated corals resembling a healthy, pre-diseased state. Further investigation is also needed for early stages of disease exposure to investigate immune responses associated with lesion formation prior to cell necrosis and death. Such efforts will allow the identification of gene pathways involved in coral and algal responses to SCTLD exposure, similarities (and differences) in immune responses among species, and will facilitate the comparisons of diseased and treated corals to determine the potential for recovery and/or antibiotic resistance following disease intervention efforts.

## Acknowledgements

We acknowledge Victoria Barker, Emily Osborne, and Katharine Egan for programmatic support in the development of this study, and Ian Combs and Matt Roy for assistance in field sampling. Coral colonies were monitored, sampled, and treated under permits from the Florida Fish and Wildlife Conservation Commission to Joshua Voss (Special Activity Licenses SAL-19-1702-SRP and SAL-19-2022-SRP). High performance computing was provided by Research Computing Services at Florida Atlantic University. This study was funded by the NOAA OAR ‘Omics Program to Joshua Voss and Michael Studivan, with additional funding

support from the Florida Department of Environmental Protection to Joshua Voss and the NOAA Coral Reef Conservation Program to Ian Enochs and Michael Studivan (#31252). This is contribution XXXX from Harbor Branch Oceanographic Institute at Florida Atlantic University.

## References

- Aeby, G. S., Ushijima, B., Campbell, J. E., Jones, S., Williams, G. J., Meyer, J. L., Häse, C., & Paul, V. J. (2019). Pathogenesis of a tissue loss disease affecting multiple species of corals along the Florida Reef Tract. *Frontiers in Marine Science*, *6*, 00678. <https://doi.org/10.3389/fmars.2019.00678>
- Aeby, G., Ushijima, B., Bartels, E., Walter, C., Kuehl, J., Jones, S., & Paul, V. J. (2021). Changing stony coral tissue loss disease dynamics through time in *Montastraea cavernosa*. *Frontiers in Marine Science*, *8*, 699075. <https://doi.org/10.3389/fmars.2021.699075>
- Aranda, M., Banaszak, A. T., Bayer, T., Luyten, J. R., Medina, M., & Voolstra, C. R. (2011). Differential sensitivity of coral larvae to natural levels of ultraviolet radiation during the onset of larval competence. *Molecular Ecology*, *20*(14), 2955–2972. <https://doi.org/10.1111/j.1365-294X.2011.05153.x>
- Becker, C. C., Brandt, M., Miller, C. A., & Apprill, A. (2021). Microbial bioindicators of stony coral tissue loss disease identified in corals and overlying waters using a rapid field-based sequencing approach. *Environmental Microbiology*, *24*, 1166–1182. <https://doi.org/10.1111/1462-2920.15718>
- Chen, H., & Boutros, P. C. (2011). VennDiagram: A package for the generation of highly-customizable Venn and Euler diagrams in R. *BMC Bioinformatics*, *12*, 35. <https://doi.org/10.1186/1471-2105-12-35>
- Combs, I. R., Studivan, M. S., Eckert, R. J., & Voss, J. D. (2021). Quantifying impacts of stony coral tissue loss disease on corals in Southeast Florida through surveys and 3D photogrammetry. *PLoS ONE*, *16*(6), e0252593. <https://doi.org/10.1371/journal.pone.0252593>
- Connelly, M. T., McRae, C. J., Liu, P.-J., Martin, C. E., & Traylor-Knowles, N. (2022). Antibiotics alter *Pocillopora* coral-Symbiodiniaceae-bacteria interactions and cause microbial dysbiosis during heat stress. *Frontiers in Marine Science*, *8*, 814124. <https://doi.org/10.3389/fmars.2021.814124>
- D’Arcy, M. S. (2019). Cell death: A review of the major forms of apoptosis, necrosis and autophagy. *Cell Biology International*, *43*, 582–592. <https://doi.org/10.1002/cbin.11137>
- Davies, S. W., Ries, J. B., Marchetti, A., & Castillo, K. D. (2018). *Symbiodinium* functional diversity in the coral *Siderastrea siderea* is influenced by thermal stress and reef environment, but not ocean acidification. *Frontiers in Marine Science*, *5*, 150. <https://doi.org/10.3389/fmars.2018.00150>
- Deutsch, J. M., Jaiyesimi, O. A., Pitts, K. A., Houk, J., Ushijima, B., Walker, B. K., Paul, V. J., & Garg, N. (2021). Metabolomics of healthy and stony coral tissue loss disease affected *Montastraea cavernosa* corals. *Frontiers in Marine Science*, *8*, 714778. <https://doi.org/10.3389/fmars.2021.714778>
- Deutsch, J. M., Mandelare-Ruiz, P., Yang, Y., Foster, G., Routhu, A., Houk, J., De La Flor, Y. T., Ushijima, B., Meyer, J. L., Paul, V. J., & Garg, N. (2022). Metabolomics approaches to dereplicate natural products from coral-derived bioactive bacteria. *Journal of Natural Products*, *85*, 462–478. <https://doi.org/10.1021/acs.jnatprod.1c01110>
- Dixon, G., Abbott, E., & Matz, M. V. (2020). Meta-analysis of the general coral stress response: *Acropora* corals show opposing responses depending on stress intensity. *Molecular Ecology*, *29*, 2855–2870. <https://doi.org/10.1111/mec.15535>
- Dixon, G. B., Davies, S. W., Aglyamova, G. A., Meyer, E., Bay, L. K., & Matz, M. V. (2015). Genomic determinants of coral heat tolerance across latitudes. *Science*, *348*, 1460–1462. <https://doi.org/10.1126/science.1261224>
- Doering, T., Wall, M., Putschim, L., Rattanawongwan, T., Schroeder, R., Hentschel, U., & Roik, A. (2021). Towards enhancing coral heat tolerance: A “microbiome transplantation” treatment using inoculations of

homogenized coral tissues. *Microbiome*, 9, 102. <https://doi.org/10.1186/s40168-021-01053-6>

Emms, D. M., & Kelly, S. (2015). OrthoFinder: Solving fundamental biases in whole genome comparisons dramatically improves orthogroup inference accuracy. *Genome Biology*, 16, 157. <https://doi.org/10.1186/s13059-015-0721-2>

Emms, D. M., & Kelly, S. (2019). OrthoFinder: Phylogenetic orthology inference for comparative genomics. *Genome Biology*, 20, 238. <https://doi.org/10.1186/s13059-019-1832-y>

Forrester, G. E., Arton, L., Horton, A., Nickles, K., & Forrester, L. M. (2022). Antibiotic treatment ameliorates the impact of stony coral tissue loss disease (SCTLD) on coral communities. *Frontiers in Marine Science*, 9, 859740. <https://doi.org/10.3389/fmars.2022.859740>

Fuess, L. E., Butler, C. C., Brandt, M. E., & Mydlarz, L. D. (2020). Investigating the roles of transforming growth factor-beta in immune response of *Orbicella faveolata*, a scleractinian coral. *Developmental and Comparative Immunology*, 107, 103639. <https://doi.org/10.1016/j.dci.2020.103639>

Fuess, L. E., Pinzon C, J. H., Weil, E., Grinshpon, R. D., & Mydlarz, L. D. (2017). Life or death: Disease-tolerant coral species activate autophagy following immune challenge. *Proceedings of the Royal Society B: Biological Sciences*, 284, 20170771. <https://doi.org/10.1098/rspb.2017.0771>

Fuess, L. E., Pinzon C., J. H., Weil, E., & Mydlarz, L. D. (2016). Associations between transcriptional changes and protein phenotypes provide insights into immune regulation in corals. *Developmental and Comparative Immunology*, 62, 17–28. <https://doi.org/10.1016/j.dci.2016.04.017>

Gonzalez-Barrios, F. J., & Alvarez-Filip, L. (2018). A framework for measuring coral species-specific contribution to reef functioning in the Caribbean. *Ecological Indicators*, 95, 877–886. <https://doi.org/10.1016/j.ecolind.2018.08.038>

Gordon, A., & Hannon, G. (2010). Fastx-toolkit. *FASTQ/A Short-Reads Preprocessing Tools (Unpublished)* [http://Hannonlab.Cshl.Edu/Fastx\\_toolkit](http://Hannonlab.Cshl.Edu/Fastx_toolkit), 5.

Griffin, D. W., Banks, K., Gregg, K., Shedler, S., & Walker, B. K. (2020). Antibiotic resistance in marine microbial communities proximal to a Florida sewage outfall system. *Antibiotics*, 9, Article 3. <https://doi.org/10.3390/antibiotics9030118>

Huerta-Cepas, J., Forslund, K., Coelho, L. P., Szklarczyk, D., Jensen, L. J., Von Mering, C., & Bork, P. (2018). Fast genome-wide functional annotation through orthology assignment by eggNOG-Mapper. *Molecular Biology and Evolution*, 34, 2115–2122. <https://doi.org/10.1093/molbev/msx148>

Huerta-Cepas, J., Szklarczyk, D., Forslund, K., Cook, H., Heller, D., Walter, M. C., Rattei, T., Mende, D. R., Sunagawa, S., Kuhn, M., Jensen, L. J., Von Mering, C., & Bork, P. (2016). eggNOG 4.5: A hierarchical orthology framework with improved functional annotations for eukaryotic, prokaryotic and viral sequences. *Nucleic Acids Research*, 44, D286–D293. <https://doi.org/10.1093/nar/gkv1248>

Jacquemot, L., Bettarel, Y., Monjol, J., Corre, E., Halary, S., Desnues, C., Bouvier, T., Ferrier-Pages, C., & Baudoux, A.-C. (2018). Therapeutic potential of a new jumbo phage that infects *Vibrio coralliilyticus*, a widespread coral pathogen. *Frontiers in Microbiology*, 9, 2501. <https://doi.org/10.3389/fmicb.2018.02501>

Johnston, M. A., Studivan, M. S., Enochs, I. C., Correa, A. M. S., Besemer, N., Eckert, R. J., Edwards, K., Hannum, R., Hu, X., Nuttall, M., O’Connell, K., Palacio-Castro, A. M., Schmahl, G. P., Sturm, A. B., Ushijima, B., & Voss, J. D. (2023). Coral disease outbreak at the remote Flower Garden Banks, Gulf of Mexico. *Frontiers in Marine Science*, 10, 1111749. <https://doi.org/10.3389/fmars.2023.1111749>

Kassambara, A., Kosinski, M., & Biecek, P. (2021). Survminer: Drawing survival curves using “ggplot2”. R package version 0.4.9.

Kauffmann, A., Gentleman, R., & Huber, W. (2009). *arrayQualityMetrics*—A bioconductor package for quality assessment of microarray data. *Bioinformatics*, 25(3), 415–416.

<https://doi.org/10.1093/bioinformatics/btn647>

Kitchen, S. A., Crowder, C. M., Poole, A. Z., Weis, V. M., & Meyer, E. (2015). *De novo* assembly and characterization of four anthozoan (Phylum Cnidaria) transcriptomes. *G3: Genes, Genomes, Genetics*, *5*, 2441–2452. <https://doi.org/10.1534/g3.115.020164>

Kolde, R. (2019). *Pheatmap: Pretty heatmaps*. R package version 1.0.12.

Koval, G., Rivas, N., D’Alessandro, M., Hesley, D., Santos, R., & Lirman, D. (2020). Fish predation hinders the success of coral restoration efforts using fragmented massive corals. *PeerJ*, *8*, e9978. <https://doi.org/10.7717/peerj.9978>

Kramer, P. R., Roth, L., & Lang, J. (2019). *Map of Stony Coral Tissue Loss Disease Outbreak in the Caribbean*. Accessed 14 Oct 2022. ArcGIS Online. [www.agrra.org](http://www.agrra.org)

Landsberg, J. H., Kiryu, Y., Peters, E. C., Wilson, P. W., Perry, N., Waters, Y., Maxwell, K. E., Huebner, L. K., & Work, T. M. (2020). Stony coral tissue loss disease in Florida is associated with disruption of host–zooxanthellae physiology. *Frontiers in Marine Science*, *7*, 576013. <https://doi.org/10.3389/fmars.2020.576013>

Langfelder, P., & Horvath, S. (2008). *WGCNA: An R package for weighted correlation network analysis*. *BMC Bioinformatics*, *9*, 559. <https://doi.org/10.1186/1471-2105-9-559>

Langmead, B., & Salzberg, S. L. (2012). Fast gapped-read alignment with Bowtie 2. *Nature Methods*, *9*, 357–359. <https://doi.org/10.1038/nmeth.1923>

Liu, S., Su, H., Pan, Y.-F., & Xu, X.-R. (2020). Spatial and seasonal variations of antibiotics and antibiotic resistance genes and ecological risks in the coral reef regions adjacent to two typical islands in South China Sea. *Marine Pollution Bulletin*, *158*, 111424. <https://doi.org/10.1016/j.marpolbul.2020.111424>

Love, M. I., Huber, W., & Anders, S. (2014). Moderated estimation of fold change and dispersion for RNA-seq data with *DESeq2*. *Genome Biology*, *15*, 550–571. <https://doi.org/10.1186/s13059-014-0550-8>

MacKnight, N. J., Dimos, B. A., Beavers, K. M., Muller, E. M., Brandt, M. E., & Mydlarz, L. D. (2022). Disease resistance in coral is mediated by distinct adaptive and plastic gene expression profiles. *Science Advances*, *8*, eabo6153. <https://doi.org/10.1126/sciadv.abo6153>

Meiling, S. S., Muller, E. M., Lasseigne, D., Rossin, A., Veglia, A. J., MacKnight, N., Dimos, B., Huntley, N., Correa, A. M. S., Smith, T. B., Holstein, D. M., Mydlarz, L. D., Apprill, A., Brandt, M. E., & Neely, K. L. (2021). Variable species responses to experimental stony coral tissue loss disease (SCTLD) exposure. *Frontiers in Marine Science*, *8*, 670829. <https://doi.org/10.3389/fmars.2021.670829>

Meyer, J. L., Castellanos-Gell, J., Aeby, G. S., Hase, C. C., Ushijima, B., & Paul, V. J. (2019). Microbial community shifts associated with the ongoing stony coral tissue loss disease outbreak on the Florida Reef Tract. *Frontiers in Microbiology*, *10*, 2244. <https://doi.org/10.3389/fmicb.2019.02244>

Mydlarz, L. D., & Harvell, C. D. (2007). Peroxidase activity and inducibility in the sea fan coral exposed to a fungal pathogen. *Comparative Biochemistry and Physiology Part A: Molecular & Integrative Physiology*, *146*, 54–62. <https://doi.org/10.1016/j.cbpa.2006.09.005>

Neely, K. L., Macaulay, K. A., Hower, E. K., & Dobler, M. A. (2020). Effectiveness of topical antibiotics in treating corals affected by stony coral tissue loss disease. *PeerJ*, *8*, 9289. <https://doi.org/10.7717/peerj.9289>

NOAA. (2018). Stony Coral Tissue Loss Disease Case Definition. *NOAA, Silver Spring, MD*, 10.

Oksanen, J., Blanchet, F. G., Kindt, R., Legendre, P., Minchin, P. R., O’Hara, R., Simpson, G., Solymos, P., Stevens, M., & Wagner, H. (2015). *Vegan: Community ecology package*. R package version 2.0-10.

Palmer, C. V. (2018). Warmer water affects immunity of a tolerant reef coral. *Frontiers in Marine Science*, *5*, 253. <https://doi.org/10.3389/fmars.2018.00253>

- Peixoto, R. S., Sweet, M., Villela, H. D. M., Cardoso, P., Thomas, T., Voolstra, C. R., Hoj, L., & Bourne, D. G. (2021). Coral probiotics: Premise, promise, prospects. *Annual Review of Animal Biosciences*, *9*, 265–288. <https://doi.org/10.1146/annurev-animal-090120-115444>
- Pinzon, J. H., Kamel, B., Burge, C. A., Harvell, C. D., Medina, M., Weil, E., & Mydlarz, L. D. (2015). Whole transcriptome analysis reveals changes in expression of immune-related genes during and after bleaching in a reef-building coral. *Royal Society Open Science*, *2*, 140214. <https://doi.org/10.1098/rsos.140214>
- Pradhan, S., Madke, B., Kabra, P., & Singh, A. L. (2016). Anti-inflammatory and immunomodulatory effects of antibiotics and their use in dermatology. *Indian Journal of Dermatology*, *61*, 469–481. <https://doi.org/10.4103/0019-5154.190105>
- Precht, W. F., Gintert, B. E., Robbart, M. L., Fura, R., & Van Woesik, R. (2016). Unprecedented disease-related coral mortality in Southeastern Florida. *Scientific Reports*, *6*, 31374. <https://doi.org/10.1038/srep31374>
- R Core Team. (2019). R: *A language and environment for statistical computing*. R Foundation for Statistical Computing, Vienna, Austria. <https://www.r-project.org/>
- Rivas, N., Hesley, D., Kaufman, M., Unsworth, J., D’Alessandro, M., & Lirman, D. (2021). Developing best practices for the restoration of massive corals and the mitigation of predation impacts: Influences of physical protection, colony size, and genotype on outplant mortality. *Coral Reefs*, *40*, 1227–1241. <https://doi.org/10.1007/s00338-021-02127-5>
- Rosales, S. M., Clark, A. S., Huebner, L. K., Ruzicka, R. R., & Muller, E. M. (2020). Rhodobacterales and Rhizobiales are associated with stony coral tissue loss disease and its suspected sources of transmission. *Frontiers in Microbiology*, *11*, 681. <https://doi.org/10.3389/fmicb.2020.00681>
- Rosales, S. M., Huebner, L. K., Clark, A. S., McMinds, R., Ruzicka, R. R., & Muller, E. M. (2022). Bacterial metabolic potential and micro-eukaryotes enriched in stony coral tissue loss disease lesions. *Frontiers in Marine Science*, *8*, 776859. <https://doi.org/10.3389/fmars.2021.776859>
- Santoro, E. P., Borges, R. M., Espinoza, J. L., Freire, M., Messias, C. S. M. A., Villela, H. D. M., Pereira, L. M., Vilela, C. L. S., Rosado, J. G., Cardoso, P. M., Rosado, P. M., Assis, J. M., Duarte, G. A. S., Perna, G., Rosado, A. S., Macrae, A., Dupont, C. L., Nelson, K. E., Sweet, M. J., ... Peixoto, R. S. (2021). Coral microbiome manipulation elicits metabolic and genetic restructuring to mitigate heat stress and evade mortality. *Science Advances*, *7*, eabg3088. <https://doi.org/10.1126/sciadv.abg3088>
- Shilling, E. N., Combs, I. R., & Voss, J. D. (2021). Assessing the effectiveness of two intervention methods for stony coral tissue loss disease on *Montastraea cavernosa*. *Scientific Reports*, *11*, 8566. <https://doi.org/10.1038/s41598-021-86926-4>
- Shoguchi, E., Beedesse, G., Hisata, K., Tada, I., Narisoko, H., Satoh, N., Kawachi, M., & Shinzato, C. (2021). A new dinoflagellate genome illuminates a conserved gene cluster involved in sunscreen biosynthesis. *Genome Biology and Evolution*, *13*, evaa235. <https://doi.org/10.1093/gbe/evaa235>
- Silva, D. P., Villela, H. D. M., Santos, H. F., Duarte, G. A. S., Ribeiro, J. R., Ghizelini, A. M., Vilela, C. L. S., Rosado, P. M., Fazolato, C. S., Santoro, E. P., Carmo, F. L., Ximenes, D. S., Soriano, A. U., Rachid, C. T. C. C., Vega Thurber, R. L., & Peixoto, R. S. (2021). Multi-domain probiotic consortium as an alternative to chemical remediation of oil spills at coral reefs and adjacent sites. *Microbiome*, *9*, 118. <https://doi.org/10.1186/s40168-021-01041-w>
- Studivan, M. S. (2022a). Mstudiva/Mcav-Cladocopium-Annotated-Transcriptome: Transcriptome annotations for *Montastraea cavernosa* and *Cladocopium* spp. (Version 3.0). *Zenodo*. <https://doi.org/10.5281/zenodo.7007997>
- Studivan, M. S. (2022b). Mstudiva/Ofav-Durusdinium-Annotated-Transcriptome: Transcriptome annotations for *Orbicella faveolata* and *Durusdinium* spp. (Version 1.0). *Zenodo*.

<https://doi.org/10.5281/zenodo.7007995>

Studivan, M. S. (2022c). mstudiva/SCTLD-intervention-transcriptomics: Stony coral tissue loss disease transmission and antibiotic intervention transcriptomics (Version 1.0). *Zenodo*. <https://doi.org/10.5281/zenodo.7308500>

Studivan, M. S. (2022d). mstudiva/tag-based-RNAseq: RNA extraction and Tag-Seq library preparation and analysis pipeline (Version 1.0). *Zenodo*. <https://doi.org/10.5281/zenodo.7007692>

Studivan, M. S., Rossin, A. M., Rubin, E., Soderberg, N., Holstein, D. M., & Enochs, I. C. (2022). Reef sediments can act as a stony coral tissue loss disease vector. *Frontiers in Marine Science*, 8, 815698. <https://doi.org/10.3389/fmars.2021.815698>

Sweet, M. J., Croquer, A., & Bythell, J. C. (2011). Dynamics of bacterial community development in the reef coral *Acropora muricata* following experimental antibiotic treatment. *Coral Reefs*, 30, 1121–1133. <https://doi.org/10.1007/s00338-011-0800-0>

Sweet, M. J., Croquer, A., & Bythell, J. C. (2014). Experimental antibiotic treatment identifies potential pathogens of white band disease in the endangered Caribbean coral *Acropora cervicornis*. *Proceedings of the Royal Society B: Biological Sciences*, 281, 20140094. <https://doi.org/10.1098/rspb.2014.0094>

Teplitski, M., & Ritchie, K. (2009). How feasible is the biological control of coral diseases? *Trends in Ecology & Evolution*, 24, 378–385. <https://doi.org/10.1016/j.tree.2009.02.008>

Therneau, T. M. (2021). *Survival: A package for survival analysis in R. Rpackage version 3.2-13*.

Thurber, R. V., Mydlarz, L. D., Brandt, M., Harvell, D., Weil, E., Raymundo, L., Willis, B. L., Langevin, S., Tracy, A. M., Ritchie, K. B., Vega Thurber, R., Mydlarz, L. D., Brandt, M., Harvell, D., Weil, E., Raymundo, L., Willis, B. L., Langevin, S., Tracy, A. M., ... Lamb, J. (2020). Deciphering coral disease dynamics: Integrating host, microbiome, and the changing environment. *Frontiers in Ecology and Evolution*, 8, 575927. <https://doi.org/10.3389/fevo.2020.575927>

Traylor-Knowles, N., Baker, A. C., Beavers, K. M., Garg, N., Guyon, J. R., Hawthorn, A., MacKnight, N. J., Media, M., Mydlarz, L. D., Peters, E. C., Stewart, J. M., Studivan, M. S., & Voss, J. D. (2022). Advances in immunity 'omics in response to coral disease outbreaks. *Frontiers in Marine Science*, 9, 952199. <https://doi.org/10.3389/fmars.2022.952199>

Traylor-Knowles, N., Connelly, M. T., Young, B. D., Eaton, K., Muller, E. M., Paul, V. J., Ushijima, B., DeMerlis, A., Drown, M. K., Goncalves, A., Kron, N., Snyder, G. A., Martin, C., & Rodriguez, K. (2021). Gene expression response to stony coral tissue loss disease transmission in *M. cavernosa* and *O. faveolata* from Florida. *Frontiers in Marine Science*, 8, 681563. <https://doi.org/10.3389/fmars.2021.681563>

Ushijima, B., Meyer, J. L., Thompson, S., Pitts, K., Marusich, M. F., Tittl, J., Weatherup, E., Reu, J., Wetzell, R., Aeby, G. S., Hase, C. C., & Paul, V. J. (2020). Disease diagnostics and potential coinfections by *Vibrio coralliilyticus* during an ongoing coral disease outbreak in Florida. *Frontiers in Microbiology*, 11, 2682. <https://doi.org/10.3389/fmicb.2020.569354>

Veglia, A. J., Beavers, K., Buren, E. W. V., Meiling, S. S., Muller, E. M., Smith, T. B., Holstein, D. M., Apprill, A., Brandt, M. E., Mydlarz, L. D., & Correa, A. M. S. (2022). Alphaflexivirus genomes in stony coral tissue loss disease-affected, disease-exposed, and disease-unexposed coral colonies in the U.S. Virgin Islands. *Microbiology Resource Announcements*, 11, e01199-21. <https://doi.org/10.1128/MRA.01199-21>

Voolstra, C. R., Schwarz, J. A., Schnetzer, J., Sunagawa, S., Desalvo, M. K., Szmant, A. M., Coffroth, M. A., & Medina, M. (2009). The host transcriptome remains unaltered during the establishment of coral–algal symbioses. *Molecular Ecology*, 18, 1823–1833. <https://doi.org/10.1111/j.1365-294X.2009.04167.x>

Walker, B. K., Turner, N. R., Noren, H. K. G., Buckley, S. F., & Pitts, K. A. (2021). Optimizing stony coral tissue loss disease (SCTLD) intervention treatments on *Montastraea cavernosa* in an endemic zone. *Frontiers*

in *Marine Science*, 8, 666224. <https://doi.org/10.3389/fmars.2021.666224>

Walton, C. J., Hayes, N. K., & Gilliam, D. S. (2018). Impacts of a regional, multi-year, multi-species coral disease outbreak in Southeast Florida. *Frontiers in Marine Science*, 5, 323. <https://doi.org/10.3389/fmars.2018.00323>

Wang, P., Bouwman, F. G., & Mariman, E. C. M. (2009). Generally detected proteins in comparative proteomics—A matter of cellular stress response? *Proteomics*, 9, 2955–2966. <https://doi.org/10.1002/pmic.200800826>

Williams, L. M., Fuess, L. E., Brennan, J. J., Mansfield, K. M., Salas-Rodriguez, E., Welsh, J., Awtry, J., Banic, S., Chacko, C., Chezian, A., Dowers, D., Estrada, F., Hsieh, Y.-H., Kang, J., Li, W., Malchiodi, Z., Malinowski, J., Matuszak, S., McTigue, T., ... Gilmore, T. D. (2018). A conserved Toll-like receptor-to-NF- $\kappa$ B signaling pathway in the endangered coral *Orbicella faveolata*. *Developmental & Comparative Immunology*, 79, 128–136. <https://doi.org/10.1016/j.dci.2017.10.016>

Work, T. M., Weatherby, T. M., Landsberg, J. H., Kiryu, Y., Cook, S. M., & Peters, E. C. (2021). Viral-like particles are associated with endosymbiont pathology in Florida corals affected by stony coral tissue loss disease. *Frontiers in Marine Science*, 8, 750658. <https://doi.org/10.3389/fmars.2021.750658>

Wright, R. M., Aglyamova, G. V., Meyer, E., & Matz, M. V. (2015). Gene expression associated with white syndromes in a reef building coral, *Acropora hyacinthus*. *BMC Genomics*, 16, 371. <https://doi.org/10.1186/s12864-015-1540-2>

Young, B. D., Serrano, X. M., Rosales, S. M., Miller, M. W., Williams, D., & Traylor-Knowles, N. (2020). Innate immune gene expression in *Acropora palmata* is consistent despite variance in yearly disease events. *PLOS ONE*, 15, e0228514. <https://doi.org/10.1371/journal.pone.0228514>

### Data Availability Statement

All sequence files associated with this study can be found in the National Center for Biotechnology Information (NCBI) Sequence Read Archive (SRA) under BioProject PRJNA897845, accession numbers SAMN31581862 through SAMN31582010. Datasets and analysis scripts generated from this study are available in a GitHub repository (Studivan, 2022c). Pipelines for bioinformatics and transcriptome annotations are described in separate GitHub repositories for Tag-Seq, *M. cavernosa*, and *O. faveolata* (Studivan, 2022d, 2022a, 2022b).

### Benefit-Sharing Statement

Benefits from this research accrue from the sharing of our data and results on public databases as described above, and through the Florida Department of Environmental Protection’s Disease Advisory Committee.

### Tables

**Table 1.** Sample sizes and transmission metrics for the transmission experiment including proportion of individuals exhibiting disease lesions (transmission rate) and the time to onset of lesions (mean time to transmission). Treatment sample size denoted by  $n_{\text{treat}}$  and the number of samples exhibiting lesions as  $n_{\text{lesion}}$ , with samples used for host and symbiont differential gene expression analyses as  $n_{\text{host}}$  and  $n_{\text{sym}}$ , respectively.

Species	Treatment	$n_{\text{treat}}$	$n_{\text{host}}$	$n_{\text{sym}}$	$n_{\text{lesion}}$	Transmission Rate	Days to Transmission
<i>Montastraea cavernosa</i>	Control	20	20	18	0	0%	N/A
	SCTLD	20	19	18	11	55%	$5.4 \pm 1.0$
<i>Orbicella faveolata</i>	Control	20	19	20	0	0%	N/A
	SCTLD	20	18	14	19	95%	$3.1 \pm 0.5$

**Table 2.** Sample sizes for the intervention experiment, where  $n_{\text{treat}}$  denotes treatment sample sizes,  $n_{\text{host}}$

and  $n_{\text{sym}}$  denote the number of samples used for host and symbiont differential gene expression analyses, respectively.

Time Point	Treatment	$n_{\text{treat}}$	$n_{\text{host}}$	$n_{\text{sym}}$
2020-04-21	Healthy	19	15	15
( $t_0$ )	Diseased	15	15	15
2020-05-04	Healthy	19	15	14
( $t_1$ )	Treated	15	15	13

**Table 3.** PERMANOVA test statistics for differential gene expression analyses by experiment, host species, and associated symbionts across treatments (disease status: healthy, diseased, nai; exposure group: control, scld). Nonsignificant  $p$  values denoted as ns.

Experiment	Species	Factor	df	F	R2	p
Transmission	<i>Montastraea cavernosa</i>	colony	19	1.9550	0.6282	<0.001
		status	2	2.4890	0.0842	<0.001
	<i>Cladocopium</i> spp.	colony	19	1.1746	0.5607	0.024
		status	2	1.7443	0.0876	0.002
	<i>Orbicella faveolata</i>	colony	19	1.2049	0.5641	0.057
		treatment	1	1.6927	0.0417	0.056
Intervention	<i>Durusdinium</i> spp.	colony	19	1.1000	0.5945	ns
		treatment	1	1.2558	0.0357	ns
	<i>Montastraea cavernosa</i>	time	1	1.2422	0.0222	ns
		treatment	1	0.9615	0.0172	ns
	<i>Cladocopium</i> spp.	time:treat	1	0.8250	0.0147	ns
		time	1	1.2322	0.022	ns
treatment		1	0.9554	0.0171	ns	
		time:treat	1	0.8264	0.0148	ns

**Table 4.** Differentially expressed genes (DEGs) by experiment, host species, and associated symbionts across treatment pairwise comparisons. Up denotes DEGs with higher relative expression in treatment x / treatment y, and Down denotes lower relative expression.

Experiment	Species	Comparison	Host DEGs	Host DEGs	Host DEGs	Sym DEGs
			Up	Down	Total	Up
Transmission	<i>Montastraea cavernosa</i>	diseased_healthy	3890	3878	7768	4
		nai_healthy	43	72	115	2
		diseased_nai	960	860	1820	0
Intervention	<i>Orbicella faveolata</i>	diseased_healthy	385	188	573	0
		<i>Montastraea cavernosa</i>	diseased0_healthy0	284	126	410
	treated1_diseased0	48	193	241	0	
	treated1_healthy1	4	1	5	0	
	healthy1_healthy0	183	65	248	8	
	treated1_healthy0	269	246	515	5	
		diseased0_healthy1	128	137	265	1

**Table 5.** Matching enriched gene ontology (GO) terms across species for the transmission experiment, separated by GO categories Molecular Function (MF), Biological Process (BP), and Cellular Component (CC). FDR-corrected  $p$  values correspond to results of Mann-Whitney  $U$  tests on pairwise contrasts of

diseased / healthy samples for each species.

---

<b>GO category</b>	<b>GO name</b>	<b>Montastraea cavernosa GO terms</b>
MF	RNA binding	GO:0003723
MF	structural constituent of ribosome	GO:0003735
BP	cytoplasmic translation	GO:0002181
BP	DNA metabolic process	GO:0006259
BP	establishment of protein localization to membrane	GO:0090150
BP	intracellular protein transport	GO:0006886
BP	meiosis I cell cycle process	GO:0061982;GO:0007127
BP	nuclear-transcribed mRNA catabolic process, nonsense-mediated decay	GO:0000184
BP	peptide biosynthetic process	GO:0006412;GO:0043043
BP	peptide metabolic process	GO:0043604;GO:0006518
BP	protein targeting	GO:0006605
BP	protein targeting to membrane	GO:0006612;GO:0045047;GO:0006613
BP	translational initiation	GO:0006413
CC	cytosolic large ribosomal subunit	GO:0022625
CC	cytosolic part	GO:0044445
CC	cytosolic ribosome	GO:0022626
CC	cytosolic small ribosomal subunit	GO:0022627
CC	large ribosomal subunit	GO:0015934
CC	polysome	GO:0005844
CC	ribonucleoprotein complex	GO:1990904
CC	ribosome	GO:0005840;GO:0044391

---

## Figures



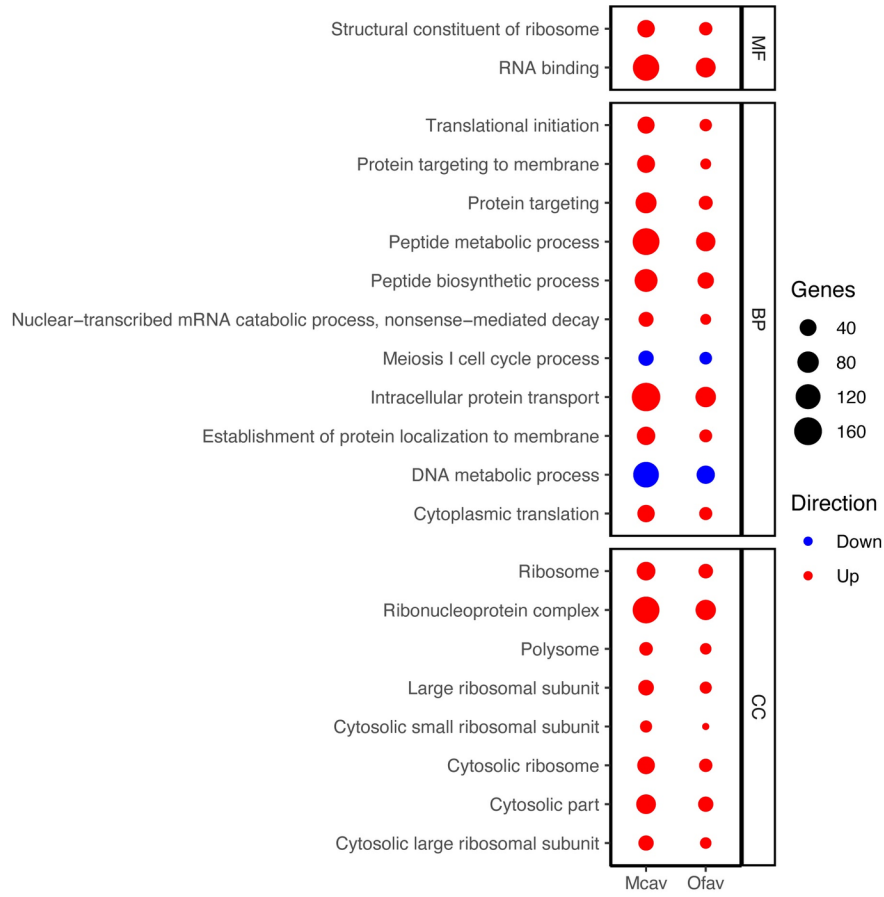


**Figure 3.** Bubble plot of matching enriched gene ontology (GO) terms across species (M cav: *M. cavernosa* ; Ofav: *O. faveolata* ) for the transmission experiment. The size of the bubble corresponds to the number of genes enriched within the GO term, the color denotes the direction of enrichment, and panels separate GO categories Molecular Function (MF), Biological Process (BP), and Cellular Component (CC).

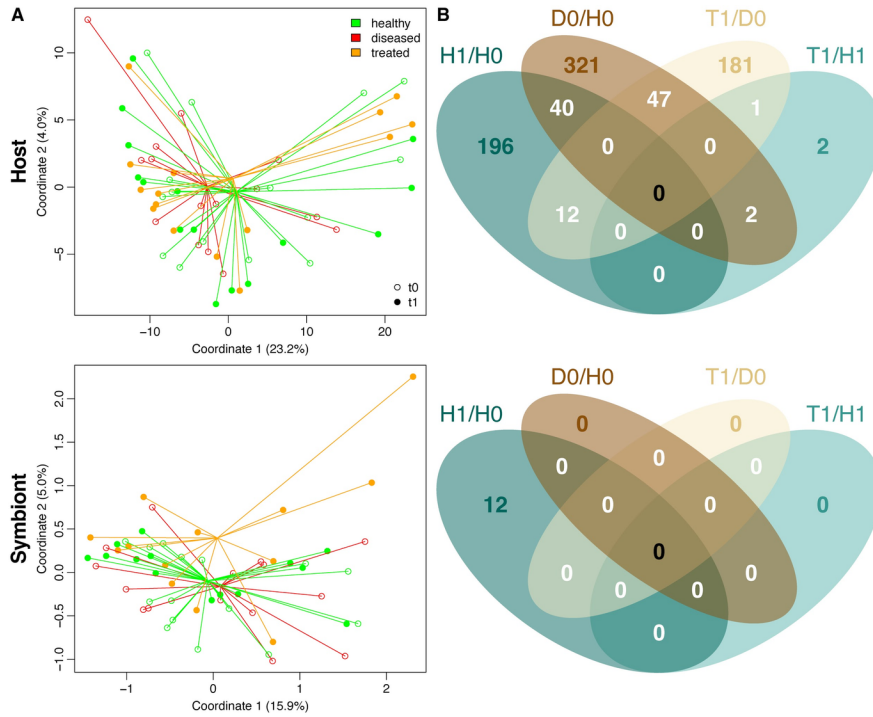


**Figure 4.** A) PCoAs of *M. cavernosa* samples and associated symbionts from the intervention experiment, visualizing sample variation among treatments (healthy, diseased, and treated; color) and sampling time points (t<sub>0</sub> and t<sub>1</sub>; shapes). Percentages indicate the amount of variation explained by the respective axis. B) Venn diagrams of common DEGs across pairwise comparisons of treatments/time (H1/H0: Healthy t<sub>1</sub>/Healthy t<sub>0</sub>; D0/H0: Diseased t<sub>0</sub>/Healthy t<sub>0</sub>; T1/D0: Treated t<sub>1</sub>/Diseased t<sub>0</sub>; T1/H1: Treated t<sub>1</sub>/Healthy t<sub>1</sub>).

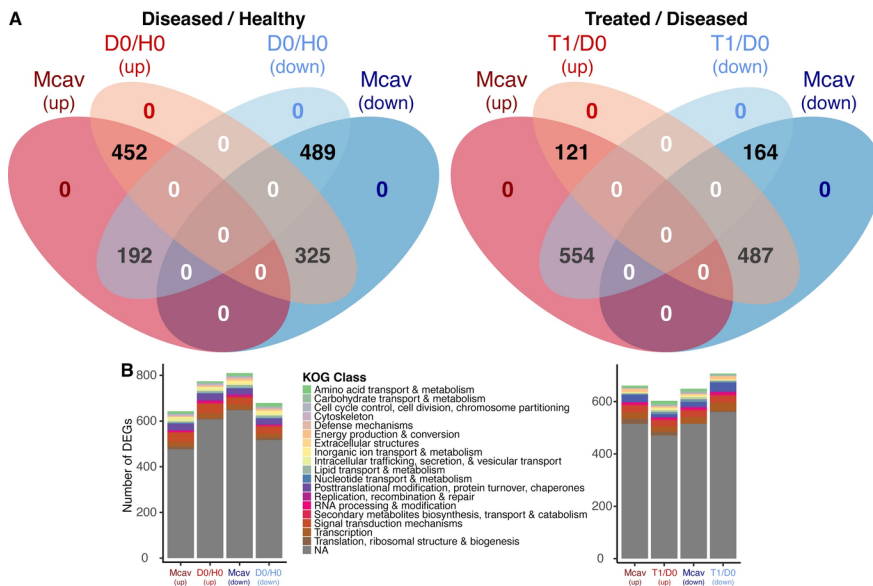


**Figure 5.** A) Common genes across pairwise treatment comparisons between transmission and intervention

experiments, denoting higher relative expression in diseased/healthy or treated/diseased as red (up), and lower expression as blue (down). C) Representation of eukaryotic orthologous groups (KOGs) across common genes for relative expression levels (up, down) and treatment comparisons (Mcav: *M. cavernosa* ; D0/H0: Diseased  $t_0$ /Healthy  $t_0$ ; T1/D0: Treated  $t_1$ /Diseased  $t_0$ ).